A finite element model of heat transport in the human eye

1988 Phys. Med. Biol. 33 227

(http://iopscience.iop.org/0031-9155/33/2/003)

Phys. Med. Biol., 1988, Vol. 33, No 2, 227-241. Printed in the UK

A finite element model of heat transport in the human eye

Jennifer A Scott

National Radiological Protection Board, Chilton, Didcot, Oxon OX11 0RQ, UK

Received 12 December 1986, in final form 7 October 1987

Abstract. A mathematical model of the human eye based on the bioheat transfer equation is developed. The intraocular temperature distribution is calculated using the Galerkin finite element method. A difficulty associated with the development of an accurate model of the human eye is the lack of reliable biological data available on the constants and parameters that are used in the model. These parameters include the thermal conductivities of the ocular tissues, the heat loss from the anterior corneal surface to the surroundings by convection and evaporation, and the convective heat loss from the sclera to the body core. The different values for the parameters reported in the ophthalmic literature are employed in the model, and the sensitivity of the temperature distribution to uncertainties in the parameters is investigated. A set of control parameter values is suggested for the normal human eye. The effect of the ambient temperature and the body-core temperature on the temperature distribution in the human eye is considered.

1. Introduction

This paper presents a mathematical model of heat transport in the human eye. This work forms part of a project to calculate the temperature rises in the human eye induced by exposure to infrared radiation. In the late nineteenth and early twentieth centuries there were reports of an increased incidence of cataracts among workers in the glass industry who were exposed to levels of infrared radiation exceeding environmental levels for prolonged periods (Meyhofer 1886, Robinson 1903, 1907, Legge 1907). Differing theories have been forwarded for the aetiology of 'glass-blowers' cataracts' (Vogt 1932, Verhoeff and Bell 1915, Goldmann 1933a, b). Whether cataracts result from a thermal effect, as widely believed, or from less well defined abiotic effects, is still not entirely clear. Nor is it clear whether infrared cataracts result from the absorption of the infrared radiation directly in the lens or in the iris, or by a combination of both. The recent research by Pitts and Cullen (1981) supports the hypothesis of Goldmann that cataracts result from infrared radiation being absorbed by the iris and the indirect transmittance of heat to the lens. Nevertheless, the controversy over the mechanisms which cause infrared cataracts remains a viable subject of debate (see, for example, Waxler and Hitchins 1986, Wolbarsht 1982).

In considering safety standards for the exposure of workers to infrared radiation it is important to be able to calculate temperature rises experienced in the human eye when exposed to infrared radiation. As a first step in that direction the temperature distribution in the normal unexposed human eye must be determined. This paper reports the results of employing a finite element model to calculate the temperature distribution in the unexposed eye; the calculation of temperature rises in the eye induced by exposure to infrared radiation will be reported in the following paper (Scott 1988).

0031-9155/88/020227+15$02.50

Models of heat transport in the eye have previously been presented in the literature. These models are briefly reviewed and assessed in § 2. Since all models of the eye are quantitative approximations of a complex physical system, appropriate values for the constants and parameters used in the models must be supplied. In all mathematical models of biological systems, finding appropriate parameter values presents a problem, and this becomes particularly important when the model is used for different subjects and different physiological and environmental conditions. Existing models tend to claim good agreement with an individual set of experimental data, which is generally for rabbit eyes, since direct experimentation with human eyes is not possible. Previous investigators have derived parameter values by fitting their measured temperature distributions for rabbit eyes to their calculated temperatures (Lagendijk 1982); this will necessarily result in the computed results for rabbits agreeing closely with the presented experimental data. The lack of detailed experimental data for human eyes makes it difficult to validate any model of the human eye.

In this study the importance of the discrepancies that exist in the parameters required in the model of the human eye is investigated by means of a sensitivity analysis. This highlights some of the parameters which must be known accurately before the temperatures calculated using the model can be considered reliable. The effects of different ambient temperatures and variations in the body-core temperature on the intraocular temperature distribution are also examined.

2. Existing eye models

One of the first models of the eye to appear in the literature was that given by Al-Badwaihy and Youssef (1976). They presented a simple heat transport model to examine the thermal effects of microwave radiation on the human eye. This model permitted an analytical method of solution for the steady-state temperature distribution. The disadvantage of this model was that to obtain an analytic solution the microwave field was assumed to decay exponentially along the axis of the eye, and the geometry and structure of the eye had to be supposed to be very simple. In particular, the eye was taken to be a spherical structure composed of a single uniform tissue. The thermal conductivity of this tissue was estimated by averaging the thermal conductivities of the various ocular tissues. The model provided some insight into the steady-state temperature distribution in the human eye when exposed to microwave radiation, but the analytic method of solution did not extend to the calculation of transient (time-varying) temperature distributions. Moreover, the effect of the lens as a thermal barrier in preventing heat flowing between the anterior and posterior regions of the eye was obscured by the averaging of the thermal conductivities. To model the eye and exposure conditions more realistically than in the work by Al-Badwaihy and Youssef a numerical method solution of the differential equations used to describe the heat transport must be adopted.

Taflove and Brodwin (1975) in their computation of the intraocular temperatures in a microwave-irradiated human eye were able to obtain transient solutions by using a finite difference method of solution. Again the assumption was made that the eye is homogeneous; the eye tissue parameters were assigned the appropriate values for water. As a result the effects of the lower thermal conductivity of the lens were lost. The model used by Taflove and Brodwin assumed that the convective heat transfer parameter used to describe the heat lost from the eye was constant over the entire surface of the eyeball; the heat loss from the cornea to the surrounding room was not distinguished from that lost across the sclera to the body core. Consequently the model did not take into account the ambient temperature, the body-core temperature, or the rate of evaporation from the anterior corneal surface. In the present study it will be seen that each of these factors has a significant effect on the temperature distribution in the human eye. In calculating transient temperatures Taflove and Brodwin took the initial temperature in the eye at time $t = 0$ to be a uniform 37 °C. This is an incorrect assumption and, since the transient solution of a time-dependent heat transport equation is dependent on the initial temperature distribution, there are errors in their calculated transient temperature profiles for the microwave-irradiated eye.

A more sophisticated model than that used by Taflove and Brodwin was presented by Emery *et al* (1975). This model was of the rabbit eye and employed a finite element method of solution. The iris and ciliary body were taken to form part of the boundary of the domain. The model was used to calculate the initial temperature distribution in the normal unexposed rabbit eye and the temperature rises induced by exposure to microwave radiation. The model was not transposed to the human eye.

Recently, mathematical models of human and rabbit eyes have been presented by Lagendijk (1982). In these models a simple explicit forward-difference heat balance technique was used. Both transient and steady-state calculations were performed. The use of an explicit method results in stability and hence convergence criteria imposing a restriction on the step size permitted in the time integration, with the maximum time step being directly related to the fineness of the finite difference (spatial) mesh. The finite difference method in general has more problems than the finite element method in accommodating the shapes of different materials within a complicated structure such as the eye. The grid used by Lagendijk can only crudely approximate the shape of the lens and the other eye structures. This approximation could be improved by a refinement of the grid, but this in turn would impose further restrictions on the maximum time step allowed. Alternatively, an implicit backward-difference or alternating-direction method could be employed. This would significantly increase the computational costs but remove the stability restriction on the time stepping data.

In the following sections a model of the human eye which employs finite elements in space combined with finite differences in time is presented. The maximum time step is only restricted by considerations of precision. The finite element mesh allows a precise representation of the ocular structures, and may be adjusted if necessary for each individual eye under examination.

3. The mathematical model

Simplifying assumptions concerning the geometry and structure of the eye must be made in order to model heat transport in the eye mathematically. A schematic cross section of the eye is given in figure 1. For the purpose of the model the eye is divided into six regions, namely cornea, aqueous humour, lens, iris, ciliary body and vitreous humour. Each region is assumed to be homogeneous. The eye is assumed to be symmetric about the pupillary axis. It is then convenient to formulate the problem in cylindrical coordinates (r, θ, z), with the z axis constituting the pupillary axis. Provided all coefficients are independent of θ, the unknown temperature T is a function of (r, z) only, and the assumption of symmetry about the pupillary axis thus allows the problem to be reduced to one of two space dimensions.

The eye's cooling mechanisms are assumed to be located at the surface of the eyeball. Heat is lost from the anterior corneal surface exposed to the surrounding air

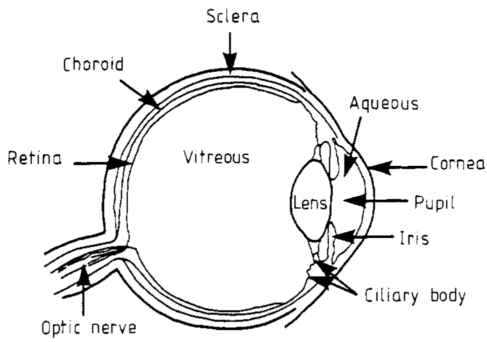

Figure 1. Schematic diagram of the eye.

by evaporation, convection and radiation. Over the remaining part of the eyeball cooling (or heating in the unexposed eye) is accomplished by means of the high blood flow in the sclera/choroid/retina region. The part of the blood flow that goes to the ciliary body and iris is included in the choroid (including sclera and retina) blood flow since this blood enters and leaves the eye through the choroid.

The slow replenishment and natural convection of the aqueous humour is assumed to have a negligible effect on heat transfer (Emery *et al* 1975, Kramar *et al* 1978).

With the above assumptions the governing differential equation for the temperature distribution is the bioheat transfer equation

$$\rho c\, \partial T/\partial t = \mathrm{div}(k \,\mathrm{grad}\, T) + H \qquad \text{in } \Omega \tag{3.1}$$

(the interior of the eyeball ($t > 0$)), with boundary conditions

$$k\, \partial T/\partial n = 0 \tag{3.2}$$

on Γ_1 (the pupillary axis)

$$-k\, \partial T/\partial n = h_s(T - T_{bl}) \tag{3.3}$$

on Γ_2 (the sclera)

$$-k\, \partial T/\partial n = E + h_c(T - T_{amb}) + \sigma\varepsilon(T^4 - T_{amb}^4) \tag{3.4}$$

on Γ_3 (the anterior corneal surface).

The initial temperature distribution is found by solving the steady-state heat transfer equation

$$\mathrm{div}(k \,\mathrm{grad}\, T) = 0 \qquad \text{in } \Omega \tag{3.5}$$

subject to the boundary conditions (3.2)-(3.4) (with $t = 0$).

In equations (3.1)-(3.5) the following notation has been used. T, unknown temperature (K); k, thermal conductivity (W m^{-1} °C^{-1}); c, specific heat capacity (J kg^{-1} °C^{-1}); ρ, density (kg m^{-3}); t, time (s^{-1}); E, evaporation rate (W m^{-2}); T_{amb}, ambient temperature (K); T_{bl}, blood temperature (K); h_s, convective heat transfer coefficient from the sclera to the body core (W m^{-2} °C^{-1}); h_c, convective heat transfer coefficient from the cornea to the surroundings (W m^{-2} °C); n, unit outward normal (m); σ, Stefan constant ($\sigma = 5.6697 \times 10^{-8}$ W m^{-2} K^{-4}); ε, emissivity of corneal surface; H, heat source (W m^{-3}).

Note that the aim of this paper is to consider only the normal temperature distribution in the unexposed human eye. Consequently in this paper the heat source is $H=0$. For the unexposed eye the temperature distribution will be constant with time so that only the steady-state temperature needs to be considered. However, it will be necessary to solve both for transient and steady-state solutions when the eye is exposed to infrared radiation. As a result the finite element method for the transient and steady-state solutions is given in the next section.

For the normal unexposed eye the effects of factors such as blinking and eyelid closure are not included in the model; these parameters will be of importance in calculating the heat source term H when considering the thermal effects of exposure to infrared radiation.

4. The numerical method

To solve equations (3.1)-(3.5) numerically a finite element discretisation in space combined with a finite difference method in time is employed. The domain Ω is divided into discrete parts (the finite elements) and the unknown function T is approximated by

$$T(r, z, t)=\sum_{i=1}^{n} N_i(r, z) T_i(t) \tag{4.1}$$

where n is the total number of nodes, $\{N_i\}$ are the global shape functions and $\{T_i(t)\}$ are the time-dependent nodal parameters.

In the Galerkin weighted residual method the $T_i(t)$ are determined to satisfy the n equations

$$\int_V \left(\rho c \frac{\partial T}{\partial t}-\operatorname{div}(k \operatorname{grad} T)-H\right) N_i \, \mathrm{d}V=0 \qquad i=1(1)n \tag{4.2}$$

(see, for example, Fletcher 1984).

Here the integration is over the axisymmetric volume V, in particular,

$$\mathrm{d}V=r \, \mathrm{d}\theta \, \mathrm{d}r \, \mathrm{d}z=r \, \mathrm{d}\theta \, \mathrm{d}\Omega$$

and since (4.2) is independent of θ,

$$\mathrm{d}V=2\pi r \, \mathrm{d}\Omega.$$

Substituting into (4.2) the Galerkin equations become

$$\int_\Omega r\left(\rho c \frac{\partial T}{\partial t}-\operatorname{div}(k \operatorname{grad} T)-H\right) N_i \, \mathrm{d}\Omega=0 \qquad i=1(1)n. \tag{4.3}$$

Using the approximation (4.1) in (4.3), employing Green's theorem and then interchanging the order of summation and integration yields the system of ordinary differential equations:

$$M \, \mathrm{d}T/\mathrm{d}t+KT+K_r(T)=f+q \qquad t>0 \tag{4.4}$$

in which $(T)_i=T_i(t)$, $i=1(1)n$, and

$$M_{ij}=\int_\Omega \rho c r N_i N_j \, \mathrm{d}\Omega \qquad i, j=1(1)n \tag{4.5}$$

$$K_{ij} = \int_\Omega kr\left(\frac{\partial N_i}{\partial r}\frac{\partial N_j}{\partial r} + \frac{\partial N_i}{\partial z}\frac{\partial N_j}{\partial z}\right) \mathrm{d}\Omega$$

$$+ \int_{\Gamma_2} h_s r N_i N_j \,\mathrm{d}\Gamma + \int_{\Gamma_3} h_c r N_i N_j \,\mathrm{d}\Gamma \qquad i, j = 1(1)n \tag{4.6}$$

$$(K_r(T))_i = \int_{\Gamma_3} r\sigma\varepsilon(T^4 - T^4_{\mathrm{amb}}) N_i \,\mathrm{d}\Omega \qquad i = 1(1)n \tag{4.7}$$

$$(f)_i = \int_{\Gamma_2} h_s r T_{\mathrm{bl}} N_i \,\mathrm{d}\Gamma - \int_{\Gamma_3} r(E - h_c T_{\mathrm{amb}}) N_i \,\mathrm{d}\Gamma \qquad i = 1(1)n \tag{4.8}$$

$$(q)_i = \int_\Omega rHN_i \,\mathrm{d}\Omega \qquad i = 1(1)n. \tag{4.9}$$

By also applying the finite element method to equation (3.5) the initial temperature distribution is found by solving the system of equations

$$KT + K_r(T) = f \tag{4.10}$$

where the entries of K, $K_r(T)$ and f are given by (4.6), (4.7) and (4.8), respectively.

The system of ordinary differential equations (4.4) may be solved numerically using the one-parameter family of methods given by

$$M[(T_{n+1} - T_n)/\Delta t] + \alpha K T_{n+1} + (1-\alpha) K T_n + K_r(T_{n+\alpha})$$
$$= \alpha(f_{n+1} + q_{n+1}) + (1-\alpha)(f_n + q_n) \qquad n = 0, 1, 2, \ldots \tag{4.11}$$

where

$$T_{n+\alpha} = \alpha T_{n+1} + (1-\alpha) T_n.$$

Here T_n denotes an approximation to $T(n\Delta t)$; f_n, q_n are defined similarly, with $q_0 = 0$. The starting value T_0 is the solution of the solution of the system (4.10). The parameter α belongs to the interval [0, 1].

It can be shown (Hughes 1977) that if $\alpha \geqslant \frac{1}{2}$ is chosen then the scheme (4.11) is unconditionally stable. This implies that stability and convergence criteria do not impose any restriction on the maximum permissible step size Δt; Δt will only be limited by accuracy considerations.

Note that the equations (4.10) and (4.11) are non-linear. The equations may be linearised by approximating the radiation heat transfer from the corneal surface by a convection boundary condition. The radiation heat transfer coefficient is defined as

$$h_r = \sigma\varepsilon(T^2 + T^2_{\mathrm{amb}})(T + T_{\mathrm{amb}}) \tag{4.12}$$

and for the range of tissue temperatures 30–45 °C and normal room temperatures h_r is approximately equal to 6 W m^{-2} °C^{-1}. Using this approximation significantly reduces the computational effort required at each time step.

5. The control parameters

There is a lack of reliable data available on the parameters required in the model (3.1)–(3.4) of the human eye. Most of the data reported in the literature were obtained from animal experiments, in particular, from experiments on rabbits and monkeys, and must be extrapolated to the human case; this will clearly involve uncertainties. In this section the control parameters that are employed in the model are discussed.

5.1. Dimensions of the eye

The dimensions of the human eye are taken from Charles and Brown (1975). The scale diagram given by Charles and Brown is for the unaccommodated eye of a normal adult and was used to produce figure 2. The pupillary axial diameter of the human eye is 25.4 mm. The contour of the lens is given by the bold solid outline and the shaded area is the approximated iris and ciliary body. If necessary the dimensions of the model eye can be adjusted for each individual eye under consideration. This may be necessary to take into account the variation in the lens thickness with age.

5.2. Physical properties of the eye media

Values of the thermal conductivity k, the specific heat capacity c and the density ρ are required for each of the six regions of the eye; these parameters are assumed constant within each region. For the cornea, aqueous humour, lens and vitreous humour the values of k, c, ρ which are taken as control values are tabulated in table 1. The values of k, c, ρ for the iris and ciliary body are assumed to be equal to those of the aqueous humour. Note that for the cornea and for the aqueous and vitreous humours the physical constants k, c, ρ are close to those of water, but the values of k and c for the lens are significantly lower. The values of k and c for the lens were determined by

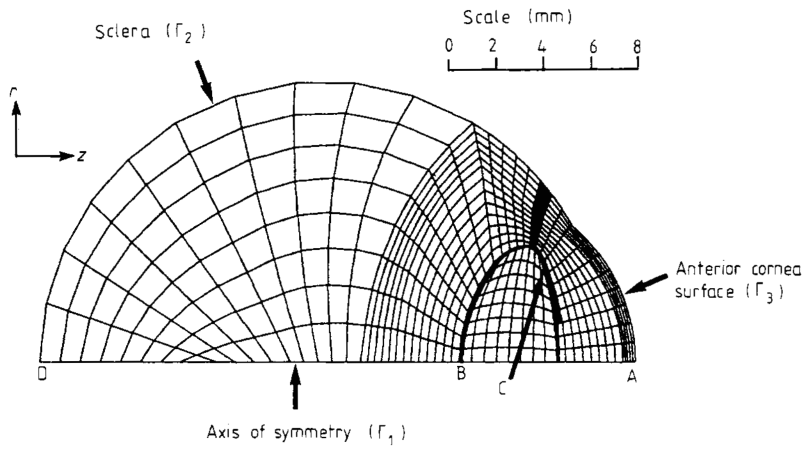

Figure 2. The finite element mesh.

Table 1. Physical constants of the ocular media.

Medium	k (W m^{-1} °C^{-1})	c (J kg^{-1} °C^{-1})	ρ (kg m^{-3})
Cornea	0.58 (Emery *et al* 1975)	4178 (water)	1050 (tissue, Neelakantaswany and Ramakrishnan 1979)
Aqueous humour	0.58 (Emery *et al* 1975)	3997 (saline solution)	1000 (water)
Lens	0.40 (Lagendijk 1982)	3000 (Lagendijk 1982)	1050 (tissue, Neelakantaswany and Ramakrishnan 1979)
Vitreous humour	0.603 (water)	4178 (water)	1000 (water)

Lagendijk (1982) using a technique of fitting calculated temperature distributions for rabbit eyes to corresponding experimental data.

5.3. *Evaporation rate*

Using the data given by Adler (1970) that 0.5–1.25 g of tears are secreted over a 16 h period, with 25% lost by evaporation, the evaporation rate E is calculated to lie in the approximate range 40–100 W m^{-2}. The lowest value $E = 40$ W m^{-2} yields the highest temperatures in the eye and is employed as the control value.

5.4. *Convective heat transfer coefficients*

The value h_c of the convective heat transfer coefficient from the anterior surface of the eyeball to the surrounding room temperature is taken to be $h_c = 10$ W m^{-2} °C^{-1}. This value was proposed by Emery *et al* (1975) (see also Kramar *et al* 1978); no other value for h_c appears in the literature.

It is interesting to observe that Lagendijk (1982) combined the evaporation, radiation and convection heat transfer on the anterior surface of the cornea to give a combined heat transfer coefficient $\tilde{h}$ where

$$\tilde{h} = E/(T - T_{amb}) + h_c + h_r. \tag{5.1}$$

Lagendijk estimated $\tilde{h}$ by fitting the calculated temperature distribution to the measured temperature distribution and obtained

$$\tilde{h} = 20(\pm 2)\ \mathrm{W\ m^{-2}\ °C^{-1}}.$$

This agrees with the value for $\tilde{h}$ that is obtained for normal tissue and room temperatures by substituting into equation (5.1) the control evaporation rate E, the control convective heat transfer coefficient h_c and the approximate radiation heat transfer coefficient $h_r = 6$ W m^{-2} °C^{-1}.

The convective heat transfer coefficient h_s from the sclera to surrounding body-core temperature is assigned the control value $h_s = 65$ W m^{-2} °C^{-1} (Lagendijk 1982).

5.5. *Other parameters*

It is assumed that the brain temperature is related to the body-core temperature, which is taken to be 37 °C. The control ambient temperature is 20 °C. The emissivity of the anterior surface of the eyeball is taken to be $\varepsilon = 0.975$; this assumes that the cornea reflects 2.5% of the radiation incident upon it (Hartridge and Hill 1915, see also Mapstone 1968).

6. Results using control parameters

In the finite element method the accuracy of the computed results is determined by the coarseness of the finite element grid. In general, the finer the grid the more accurate the results but the greater the computation time. A grid of four-noded isoparametric quadrilateral elements with a total of 496 nodes was employed, as illustrated in figure 2. A check on the results was made using a heat balance. In the steady state the total heat lost across the boundaries should be equal to the heat generated within the eye, which for the normal unexposed eye is zero. In addition the program was checked using a series of test problems for which analytic results were known; good agreement was observed between analytic and computed results.

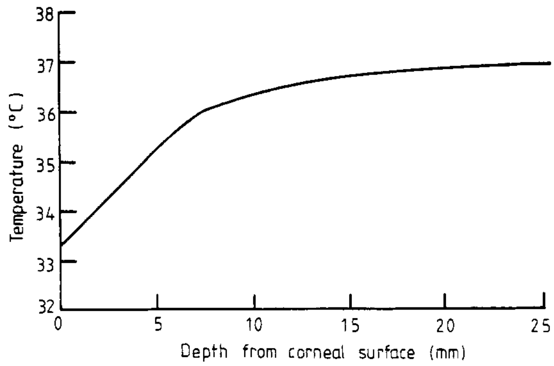

Figure 3. Temperatures along the central axis of the human eye.

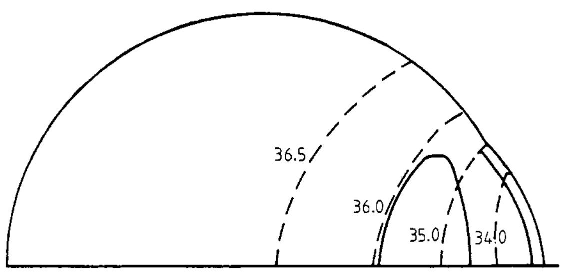

Figure 4. Steady-state isothermal contours for a normal human eye (diameter 25.4 mm).

The steady-state temperatures calculated using the control parameter values along the axis of symmetry are plotted in figure 3. The axis of symmetry was chosen as it is away from the cooling mechanisms and the highest temperatures are expected to occur along it; this expectation was confirmed by the computed results. There and throughout the remainder of the paper, temperatures are given in °C. In figure 4 the isothermal contours in the normal human eye are plotted.

It is observed that the temperature rises steeply through the cornea, aqueous humour and lens, and then levels off through the vitreous humour. The lower thermal conductivity of the lens compared with the surrounding media means that the lens prevents significant heat flow from the posterior to the anterior regions of the eye.

7. Sensitivity analysis

In this section the effects of perturbations in the control parameters given in § 5 are discussed. The aim is to determine the extent to which the temperature distribution is sensitive to different parameters; further data on these parameters for human eyes are required if confidence is to be placed in the calculated results. Values of the parameters which have been proposed in the literature but which were not assigned as control parameters are considered.

Tables 2–8 display the results of the sensitivity analysis; the points A, B, C, D are the intersection of the anterior corneal surface with the axis of symmetry, a point on the germinative zone, the posterior pole of the lens and the intersection of the retina surface with the axis of symmetry, respectively (see figure 2).

When varying a control parameter all other parameters are assigned their control values unless otherwise stated.

7.1. *Effect of thermal conductivity*

The water content of the eye lens decreases with age resulting in a decrease in its thermal conductivity, which is likely to have some effect on the temperature distribution within the eye. Values of the thermal conductivity of the lens which appear in the literature are $k = 0.21$ (Emery *et al* 1975) and $k = 0.544\ \mathrm{W\,m^{-1}\,°C^{-1}}$ (Neelakantaswamy and Ramakrishnan 1979). Results for $k = 0.21$, 0.30, 0.544 $\mathrm{W\,m^{-1}\,°C^{-1}}$ and the control value, $k = 0.40\ \mathrm{W\,m^{-1}\,°C^{-1}}$, are given in table 2.

Table 2. The effect of the thermal conductivity of the lens on the temperature distribution within the eye.

k(lens) ($\mathrm{W\,m^{-1}\,°C^{-1}}$)	A (°C)	B (°C)	C (°C)	D (°C)
0.21	33.01	35.01	36.14	36.89
0.30	33.16	35.12	36.07	36.89
0.40 (control)	33.25	35.20	36.01	36.89
0.544	33.36	35.28	35.95	36.89

Increasing the values of the thermal conductivities of the aqueous humour, cornea, iris and ciliary body to those of water was found to have little effect on the temperatures; the maximum change in the temperature was 0.05 °C, which occurred on the mid-corneal surface.

7.2. *Effect of evaporation*

The precorneal tear film is thought to be a three-layered structure. On the surface of the corneal epithelium is a thin mucoid layer; a thick aqueous layer which covers the epithelium is covered by an extremely thin oily layer produced by the Meibomian glands (Iwata *et al* 1969). The oily layer has been shown to retard evaporation from the eye. Values of the rate of evaporation in a normal eye range from 2.8 (Mishima and Maurice 1961) to 14.7 $\mathrm{mg\,h^{-1}\,cm^{-2}}$ (Adler 1970), from which E is calculated to lie in the approximate range 20–100 $\mathrm{W\,m^{-2}}$. When the oil layer of the tear film is destroyed the evaporation rate may increase to 47 $\mathrm{mg\,h^{-1}\,cm^{-2}}$, which gives $E = 320\ \mathrm{W\,m^{-2}}$ (Mishima and Maurice 1961).

Four cases are considered: the control $E = 40\ \mathrm{W\,m^{-2}}$, the minimum and maximum recorded values for a normal eye ($E = 20$ and $E = 100\ \mathrm{W\,m^{-2}}$) and the value corresponding to the oil layer having been destroyed ($E = 320\ \mathrm{W\,m^{-2}}$). Results are presented in table 3. The evaporation rate is observed to be a significant factor governing the temperature distribution in the anterior regions of the eye.

7.3. *Effect of blood flow in choroid*

A discussion of the uncertainty in the convective heat transfer coefficient h_s from the sclera to the body core is given by Lagendijk (1982). The coefficient h_s is strongly dependent on the blood flow through the eye. If it is assumed that the blood enters the eye at body-core temperature and exits at the choroidal temperature, the heat flow

Table 3. The effect of the rate of evaporation from the cornea on the temperature distribution within the eye.

E ($\mathrm{W\,m^{-2}}$)	A (°C)	B (°C)	C (°C)	D (°C)
20	33.49	35.31	36.07	36.90
40 (control)	33.25	35.20	36.01	36.89
100	32.53	34.85	35.82	36.87
320	29.88	33.58	35.13	36.79

heat flow per surface unit of the choroid is given by

$$q = (\dot{m}c_{\mathrm{bl}}/A)(T_{\mathrm{bl}} - T_{\mathrm{r}})$$

where m is the blood-flow rate in $\mathrm{kg\,s^{-1}}$ per eye, c_{bl} is the specific heat capacity of blood, A is the total area of the choroid (including the retina and sclera) and T_{bl}, T_{r} are the temperatures of the blood and retina, respectively. This heat flow may be described by the heat transfer coefficient h_{s} where

$$h_{\mathrm{s}} = q/(T_{\mathrm{bl}} - T_{\mathrm{r}}) = \dot{m}c_{\mathrm{bl}}/A.$$

Data for blood flow rates in rabbit and monkey eyes are given in O'Day *et al* (1971). Using these data Lagendijk (1982) derives an estimate $h_{\mathrm{s}} = 110\ \mathrm{W\,m^{-2}\,°C^{-1}}$. This is considerably higher than the control value $h_{\mathrm{s}} = 65\ \mathrm{W\,m^{-2}\,°C^{-1}}$ which Lagendijk found by experimentation on rabbits. The difference is probably due to the simplifying assumptions that are made regarding the blood flow in the eye. To assess the importance of the value of the coefficient h_{s}, and hence how significant the simplifying assumptions are, the values $h_{\mathrm{s}} = 65$, 90, $110\ \mathrm{W\,m^{-2}\,°C^{-1}}$ are employed (table 4).

For the unexposed eye the temperature distribution in the vitreous humour is seen to be little affected by the heat transfer coefficient h_{s} but is governed more by the blood temperature (see § 7.6). By contrast, the irradiated eye must transfer the energy absorbed in the vitreous humour, and the temperature within the vitreous humour is determined by both the blood temperature and the blood-flow rate. Thus knowledge of the value of the parameter h_{s} is likely to be of greater importance for the irradiated eye than for the unexposed eye.

7.4. *Effect of convection from cornea*

The only value for the convective heat transfer coefficient h_{c} from the cornea to the surrounding room given in the literature is that used by Emery *et al* (1975) for rabbits, i.e. $h_{\mathrm{c}} = 10\ \mathrm{W\,m^{-2}\,°C^{-1}}$. This value is taken as the control value. In addition, a reduced rate of $8\ \mathrm{W\,m^{-2}\,°C^{-1}}$ and increased rates of 12 and $15\ \mathrm{W\,m^{-2}\,°C^{-1}}$ are considered (table 5).

Table 4. The effect of the convective heat transfer coefficient from the sclera to the surrounding body core on the temperature distribution within the eye.

h_{s} ($\mathrm{W\,m^{-2}\,°C^{-1}}$)	A (°C)	B (°C)	C (°C)	D (°C)
65 (control)	33.25	35.20	36.01	36.89
90	33.38	35.34	36.13	36.93
110	33.45	35.43	36.19	36.95

Table 5. The effect of the convective heat transfer coefficient from the cornea to the surrounding room on the temperature distribution within the eye.

h_c ($\mathrm{W\,m^{-2}\,°C^{-1}}$)	A (°C)	B (°C)	C (°C)	D (°C)
8	33.58	35.36	36.10	36.90
10 (control)	33.25	35.20	36.01	36.89
12	32.92	35.04	35.92	36.88
15	32.46	34.81	35.80	36.86

7.5. Effect of ambient temperature

Heat loss from the corneal surface depends on the temperature difference between the eye tissue and the surrounding air. The temperature in an industrial environment will in general be higher than the control value of 20 °C. It is therefore of interest to investigate the effect of the ambient temperature on the temperature levels within the eye. Three cases are considered: the control value of 20 °C, and increased values of 25 and 30 °C. The results are presented in table 6. The ambient temperature is seen to have a marked effect on the temperatures in the anterior regions but to have almost no direct effect on the retinal temperature.

7.6. Effect of blood temperature

The blood flow in the choroid acts as the major source of heat for the unexposed eye (and a primary source of cooling for the irradiated eye). Consequently the blood temperature significantly affects the temperature throughout the eye. The physiological response of workmen in hot environments depends on the kind of work performed. For instance, the rectal temperature of a fit young adult performing light work (e.g., bench work) is around 37.7 °C. For moderate work (e.g., pushing and lifting) a rectal temperature of 38 °C has been suggested, and this may increase to 38.3 °C for heavy work (e.g., pick and shovel work). The descriptions of glass-working practices at the beginning of this century suggest that the work undertaken was moderate/heavy and a body-core temperature of between 38 and 38.5 °C would appear to be reasonable. In addition to the control case (37 °C), three values for the blood temperature are employed: 37.7, 38 and 38.5 °C. Results are given in table 7.

7.7. Extreme cases

At prescribed ambient and blood temperatures the possible range of parameters used in the model may be assessed by taking the worst combination of the extreme values

Table 6. The effect of the ambient temperature on the temperature distribution within the eye.

T_{amb} (°C)	A (°C)	B (°C)	C (°C)	D (°C)
20 (control)	33.25	35.20	36.01	36.89
25	34.19	35.65	36.26	36.92
30	35.15	36.11	36.51	36.94

Table 7. The effect of the blood temperature on the temperature distribution within the eye.

T_{bl} (°C)	A (°C)	B (°C)	C (°C)	D (°C)
37.0 (control)	33.25	35.20	36.01	36.89
37.7	33.81	35.83	36.67	37.58
38.0	34.05	36.10	36.96	37.88
38.5	34.45	36.55	37.43	38.38

Table 8. The effect on the calculated distribution within the eye of using extreme combinations of the parameter values.

k(lens) ($W\,m^{-1}\,°C^{-1}$)	E ($W\,m^{-2}$)	h_s ($W\,m^{-2}\,°C^{-1}$)	A (°C)	B (°C)	C (°C)	D (°C)
0.21	100	65	32.24	34.63	35.97	36.86
0.544	100	65	32.66	34.95	35.75	36.86
0.21	20	110	33.46	35.36	36.36	36.96
0.544	20	110	33.78	35.60	36.19	36.96
Control values			33.25	35.20	36.01	36.89
Variation in temperature			1.54	1.03	0.39	0.10
Mean temperature			33.01	35.09	36.16	36.91

of the parameters. Assuming that the oily layer of the tear film is not destroyed and that $h_c = 10\ W\,m^{-2}\,°C^{-1}$, the lowest temperatures in the anterior regions of the eye are calculated using $h_s = 65\ W\,m^{-2}\,°C^{-1}$, $E = 100\ W\,m^{-2}$ and $k(\text{lens}) = 0.21\ W\,m^{-1}\,°C^{-1}$; the lowest temperatures in the posterior regions are calculated using $h_s = 65\ W\,m^{-2}\,°C^{-1}$, $E = 100\ W\,m^{-2}$ and $k(\text{lens}) = 0.544\ W\,m^{-1}\,°C^{-1}$. The highest temperatures in the anterior regions are calculated using $h_s = 110\ W\,m^{-2}\,°C^{-1}$, $E = 20\ W\,m^{-2}$ and $k(\text{lens}) = 0.544\ W\,m^{-1}\,°C^{-1}$; the highest temperatures in the posterior regions are calculated using $h_s = 110\ W\,m^{-2}\,°C^{-1}$, $E = 20\ W\,m^{-2}$ and $k(\text{lens}) = 0.21\ W\,m^{-1}\,°C^{-1}$. The results (with an ambient temperature of 20 °C and a blood temperature of 37 °C) for these extreme combinations of parameters are presented in table 8. The mean of the minimum and maximum values of the temperatures at each point A, B, C, D are also included in this table. The temperature at A is most sensitive to perturbations in the control parameters, and this sensitivity decreases steadily towards the retina. The difference between the temperatures obtained using the control parameters and the mean temperatures is less than 0.25 °C. This confirms the choice of control parameters.

A major difficulty in justifying the choice of any set of control parameters is the lack of experimental data in the ophthalmic literature on the temperatures within the human eye. For an unexposed human eye mean corneal temperatures ranging from 32.06 to 34.8 °C have been recorded (Hill and Leighton 1965, Mapstone 1968). The caluclated temperatures on the cornea obtained using the extreme parameter combinations lie well within this range.

8. Deficiencies of the model

It is recognised that there are certain deficiencies in the thermal model of the eye that has been presented in this study. For example, the model has not taken into account the separate blood flow in the iris and ciliary body; blood flow has been assumed only in the sclera/choroid/retina region. There is a lack of data available on the blood flow rates within the iris and ciliary body, and the way in which the blood flow in these structures should be incorporated into the model is not at present fully understood. Lagendijk (1984) discusses some of the disadvantages and errors associated with the standard technique of incorporating blood flow in tissues into biological thermal models by including in the bioheat transfer equation a heat sink term which assumes blood enters the tissue at body-core temperature and leaves at local tissue temperature. In addition the current model has not taken into consideration the complex structure of the discrete blood vessels within the sclera. Again the uncertainty in the blood flow rates in the vessels together with the lack of knowledge of the heat flux from the vessel wall to the blood make it impossible at present to develop a model to incorporate these refinements.

The model has not been validated by experiments on humans. The impossibility of conducting experiments on human eyes makes a reliable mathematical model of heat transport in the eye essential. To this end this study has assessed the importance of the uncertainties that exist in the parameters required in any model of the human eye.

9. Concluding discussion

A finite element model of heat transport in the human eye has been developed and employed to calculate the steady-state temperature distribution in a normal human eye. This is the first stage in a study to calculate the steady-state and transient temperature distributions in the human eye when exposed to infrared radiation. The importance of obtaining reliable values for the temperature distribution in the normal human eye is that these values can be used as a set of reference temperatures with which the temperatures in an irradiated human eye can be compared. Other applications where a set of reference temperatures for the normal human eye are required include the temperature rises due to microwave radiation and the effects of eyelid closure and wind.

The main difficulty in obtaining reliable results is the lack of knowledge of the values of some of the parameters in the mathematical model. To assess the effects of uncertainties in the parameter values on the computed results a sensitivity analysis has been performed. It was found that perturbations in the thermal conductivity of the lens and in the choroidal blood flow rate lead to significant changes in the temperature in the anterior regions. A further problem is that the evaporation rate is never uniquely defined but has a considerable cooling effect, even on the normal eye. In addition, the temperature distribution was observed to be sensitive to variations in the ambient temperature and the blood temperature. Consequently, when considering the effects of infrared radiation on the intraocular temperature distribution of workers in an industrial environment it is important to have an accurate knowledge of the ambient factory temperature and an estimate of the workers' blood temperature.

Résumé

Modèle des éléments finis pour le transport de chaleur dans l'oeil humain.

L'auteur développe dans ce travail un modèle mathématique de l'oeil humain reposant sur l'équation de transfert biotherme. La distribution de température intraoculaire est calculée à l'aide de la méthode des éléments finis de Galerkin. Le manque de données biologiques fiables constitue une difficulté pour le choix des constantes et des paramètres nécessaires à l'élaboration d'un modèle précis de l'oeil humain. Ces paramètres comprennent les conductivités thermiques des tissus oculaires, les pertes de chaleur externes de la surface cornéenne antérieure par convection et évaporation, et la perte de chaleur convective de la sclérotique vers l'intérieur de l'organisme. Les différentes valeurs rapportées pour ces paramètres dans la littérature ophtalmologique ont été utilisées avec le modèle, et l'auteur a étudié la dépendance des distributions de température vis-à-vis de l'incertitude qui affecte les paramètres. Il suggère un ensemble de valeurs de paramètres de référence pour l'oeil humain normal. Il a également pris en considération l'effet de la température ambiante et de la température corporelle sur la distribution des températures dans l'oeil humain.

Zusammenfassung

Ein Modell aus endlich vielen Elementen zur Bestimmung des Wärmetransportes im menschlichen Auge.

Ein mathematisches Modell des menschlichen Auges auf der Grundlage der Biowärmetransfergleichung wurde entwickelt. Die intraokulare Temperaturverteilung wird berechnet mit Hilfe der Galerkin-Elementenmethode. Eine Schwierigkeit bei der Entwicklung eines genauen Modells des menschlichen Auges ist der Mangel an zuverlässigen biologischen Daten über die im Modell verwendeten Konstanten und Parameter. Zu diesen Parametern gehören auch die Wärmeleitfähigkeit des okularen Gewebes, die Wärmeabgabe der vorderen Corneaoberfläche an das umgebende Gewebe durch Konvektion und Verdamfung und die konvektive Wärmeabgade der Sklera an den Körper. Die verschidenen Werte, die für diese Parameter in der Literatur angegeben werden, wurden in das Modell eingearbeitet und die Empflindlichkeit der Temperaturverteilung gegenüber Parameterunsicherheiten wirden untersucht. Eine Reihe von Kontrollparameterwerten für das normale menschliche Auge wird vorgeschlagen. Der Einfluß der umgebenden Temperatur und der Körperkerntemperatur auf die Temperaturverteilung im menschlichen Auge wurde berücksichtigt.

References

Adler F H 1970 *Physiology of the Eye* 5th edn (St. Louis: Mosby)
Al-Badwaihy K A and Youssef A B A 1976 *Biological Effects of Electromagnetic Waves* vol 1, ed C C Johnson and M L Shore HEW Publication 77-8010, pp 61–78
Charles M W and Brown N 1975 *Phys. Med. Biol.* **20** 202–18
Emery A F, Kramar P O, Guy A W and Lin J C 1975 *J. Heat Transfer* C **97** 123–8
Fletcher C A J 1984 *Computational Galerkin Methods* (Berlin: Springer)
Goldmann H 1933a *Arch. Ophth.* **9** 314–6
—— 1933b *Graefes Arch. Ophth.* **130** 93–179
Hartridge H and Hill A V 1915 *Proc. R. Soc.* B **89** 58–76
Hill R M and Leighton A J 1965 *Am. J. Optom.* **42** 9–16
Hughes T J R 1977 *Comput. Meth. Appl. Mech. Eng.* **10** 135–9
Iwata S, Lemp M A, Holly F J and Dohlman C H 1969 *Invest. Ophth.* **8** 613–9
Kramar P O, Harris C, Emery A F and Guy A W 1978 *J. Microwave Power* **13** 239–49
Lagendijk J J W 1982 *Phys. Med. Biol.* **27** 1301–11
—— 1984 *PhD thesis* University Hospital Utrecht, Netherlands
Legge T M 1907 *Cataract in Glass-blowers* Home Office Report (London: HMSO)
Mapstone R 1968 *Exp. Eye Res.* **7** 237–43
Meyhofer W 1886 *Klin. Monatsbl. Augenh.* **24** 49–67
Mishima S and Maurice D 1961 *Exp. Eye Res.* **1** 46–52
Neelakantaswamy P S and Ramakrishnan K P 1979 *J. Biomech.* **12** 205–10
O'Day D M, Fish M B, Aronson S B, Pollycove M and Coon A 1971 *Arch. Ophth.* **86** 205–9
Pitts D G and Cullen A P 1981 *Graefes Arch. Klin. Exp. Ophth.* **217** 285–97
Robinson W 1903 *Br. Med. J.* **1** 191–3
—— 1907 *Br. Med. J.* **2** 381–4
Scott J A 1988 *Phys. Med. Biol.* **33** 243–57
Taflove A and Brodwin M E 1975 *IEEE Trans. Microwave Theory Tech.* **MTT-23** 888–96
Verhoeff F H and Bell L 1915 *Proc. Natl. Acad. Sci.* **51** 627–818
Vogt A 1932 *Klin. Montasbl. Augenh.* **89** 256
Waxler M and Hitchins V M (ed) 1986 *Optical Radiation and Visual Health* (Boca Raton, FL: Chemical Rubber Company)
Wolbarsht M L 1982 *Proc. Symp. Medical Ophthalmic Surveillance of Personnel Potentially Exposed to Laser Radiation* ed W G Potts and D H Sliney pp 81–8